The fractions of short- and long-range connections in the visual cortex

Armen Stepanyants[a,1], Luis M. Martinez[b], Alex S. Ferecskó[c,d], and Zoltán F. Kisvárday[e]

[a]Department of Physics and Center for Interdisciplinary Research on Complex Systems, Northeastern University, Boston, MA 02115; [b]Instituto de Neurociencias de Alicante, CSIC-UMH, 03550 Sant Joan d'Alacant, Spain; [c]Centre de Recherche Université Laval Robert-Giffard, Laval University, Quebec, Canada G1J 2G3; [d]Department of Neurophysiology, Division of Neuroscience, The Medical School, University of Birmingham, Birmingham B15 2TT, United Kingdom; and [e]Department of Anatomy, Histology, and Embryology, University of Debrecen, 4032 Debrecen, Hungary

Edited by Charles F. Stevens, The Salk Institute for Biological Studies, La Jolla, CA, and approved December 24, 2008 (received for review October 21, 2008)

When analyzing synaptic connectivity in a brain tissue slice, it is difficult to discern between synapses made by local neurons and those arising from long-range axonal projections. We analyzed a data set of excitatory neurons and inhibitory basket cells reconstructed from cat primary visual cortex in an attempt to provide a quantitative answer to the question: What fraction of cortical synapses is local, and what fraction is mediated by long-range projections? We found an unexpectedly high proportion of nonlocal synapses. For example, 92% of excitatory synapses near the axis of a 200-μm-diameter iso-orientation column come from neurons located outside the column, and this fraction remains high—76%—even for an 800-μm ocular dominance column. The long-range nature of connectivity has dramatic implications for experiments in cortical tissue slices. Our estimate indicates that in a 300-μm-thick section cut perpendicularly to the cortical surface, the number of viable excitatory synapses is reduced to about 10%, and the number of synapses made by inhibitory basket cell axons is reduced to 38%. This uneven reduction in the numbers of excitatory and inhibitory synapses changes the excitation–inhibition balance by a factor of 3.8 toward inhibition, and may result in cortical tissue that is less excitable than in vivo. We found that electrophysiological studies conducted in tissue sections may significantly underestimate the extent of cortical connectivity; for example, for some projections, the reported probabilities of finding connected nearby neuron pairs in slices could understate the in vivo probabilities by a factor of 3.

axon | connectivity | local | slice

When examining drawings (1) and 3-dimensional reconstructions (2, 3) of cortical excitatory neurons, it is difficult to evade the impression that most of the excitatory neurons' axons, and, consequently, most of their synapses, are confined to a few hundred micrometer columnar domains surrounding the neurons' somata (Fig. 1*A*). Only a few branches occasionally escape through the boundaries of the local domain. This interpretation of neuron images can be misleading, however. The few axonal branches that extend beyond the local domain could ramify over large territories (e.g., the entire cortex) and thus could carry a significant fraction of all synapses. Such long-range projections may include interareal and intraareal connections, feedback from higher cortical areas, interhemispheric projections, and feed-forward inputs from subcortical structures. These projections can be easily observed with single neuron or bulk injections of tracers (4–6), but quantifying their fraction is difficult. This is because an accurate estimate of the amount of long-range axons must be made on the scale of the entire cortex, which presents a significant challenge. In practice, long-range axons are truncated in the reconstruction process, and thus their length and richness (density), and the number of synapses that they mediate, cannot be estimated reliably.

We devised an approach to delineate the fractions of local and long-range synaptic connections in different cortical layers. Our method is based on an analysis of dendritic and local axonal arbors of 24 excitatory neurons (20 pyramidal and 4 spiny stellate) and 17 inhibitory basket cells (7, 8) labeled in vivo at different depths spanning the entire thickness of the cat primary visual cortex (area 17). We reconstructed neurons from multiple tissue sections [supporting information (SI) Fig. S1], which allowed us to recover all of the dendritic arbors and inhibitory basket cell axonal arbors in their entirety (2). But axonal branches of excitatory neurons extending beyond 1 mm from the neurons' somata in the cortical plane were truncated; thus, we have good knowledge of dendritic and local axonal arbors of neurons spanning the entire thickness of the cortex, yet little or no information about the long-range projections of excitatory neurons. Using techniques developed previously (2, 9, 10), we put together the reconstructed arbors (in numbers specified by densities of neurons in different cortical layers) and determined the densities of local synaptic connections in different cortical layers. To delineate the fractions of local and long-range excitatory synaptic connections, we compared the densities of local connections and asymmetric synapses obtained from previous electron microscopy studies of cat area 17.

Much of the experimental neuroscience research is done in 300- to 500-μm brain tissue sections. But how much of synaptic connectivity remains intact after cortical tissue is sliced? Because the sizes of dendritic and axonal arbors of cortical neurons are on the order of or much larger than the typical section thickness, a substantial tissue slicing artifact can be expected. Our experimental framework allowed us to provide a quantitative estimate of this effect by calculating the fractions of intact excitatory and inhibitory synapses, that is, synapses that remain linked to the presynaptic and postsynaptic cells of their origins after the tissue is sliced. With the overall reduction in the number of intact synapses, connections between pairs of neurons in slices are altered as well. As a result, the numbers of synapses between synaptically connected pairs of neurons (11) and the probability of finding synaptically connected pairs of neurons (12) observed in tissue slice experiments may significantly underestimate the in vivo connectivity.

Results

Connectivity Within a Cortical Column. We began our analysis by calculating the volume densities of dendritic spines of excitatory neurons in different cortical layers. Dendritic spines in a given cortical layer may originate from local neurons as well as neurons in other layers; thus, an accurate estimate of the volume density of dendritic spines must take into account details of dendritic

Author contributions: A.S., L.M.M., and Z.K.F. designed research; A.S. performed research; A.S.F. contributed new reagents/analytic tools; A.S. analyzed data; and A.S., L.M.M., A.S.F., and Z.F.K. wrote the paper.

The authors declare no conflict of interest.

This article is a PNAS Direct Submission.

[1]To whom correspondence should be addressed. E-mail: a.stepanyants@neu.edu.

This article contains supporting information online at www.pnas.org/cgi/content/full/0810390106/DCSupplemental.

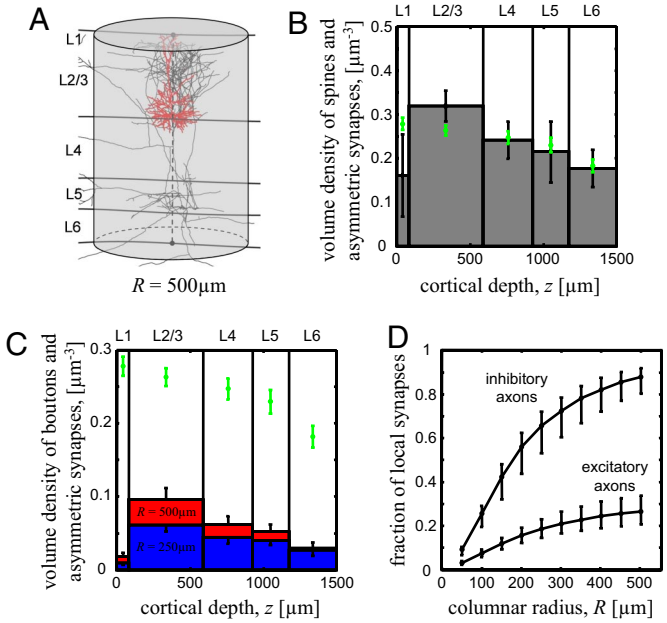

Fig. 1. Local and long-range synapses in the cortical column. (*A*) Example of a layer 2/3 pyramidal cell reconstructed from cat area 17. The axon is shown in black, and dendrites are in red. The gray cylinder (radius $R = 500\ \mu m$) demarcates the extent of the local axonal arbor. (*B*) The average volume densities of excitatory dendritic spines in different cortical layers. The green points denote the corresponding densities of asymmetric synapses. (*C*) The volume densities of boutons on local axons of excitatory neurons calculated based on 2 definitions of locality: columnar domain radii $R = 250\ \mu m$ (blue bars) and $R = 500\ \mu m$ (red bars). The green points denote the densities of asymmetric synapses for comparison. (*D*) Fractions of local synapses mediated by excitatory and inhibitory axons for different local columnar domain radii, *R*. Error bars in *B* and *C* indicate SDs; error bars in *D* show 95% CIs.

morphology of neurons belonging to different cortical layers. To calculate the volume density of dendritic spines *in silico*, we put together reconstructed dendrites according to their original laminar positions in the cortical template. Then the cortical template was tiled horizontally with the dendritic arbors in the numerical densities in which excitatory neurons appear in different cortical layers (for details, see *SI Text*). We distributed dendritic spines on all of the dendritic branches according to the frequencies in which they appear in cat area 17, and then calculated the volume densities of dendritic spines at different cortical depths. The results of these calculations are shown in Fig. 1*B*. In this figure, bars represent the volume densities of dendritic spines of excitatory neurons in different cortical layers. Layer 2/3 has the largest density of dendritic spines, $0.32 \pm 0.03\ \mu m^{-3}$, indicating that this layer contains roughly 1 dendritic spine per every $3\ \mu m^3$ of cortical gray matter. The volume density of dendritic spines decays gradually from layer 2/3 toward the deeper layers.

To verify that our sample of cortical neurons is representative and that our quantitative method is adequate, we compared the calculated volume densities of dendritic spines in different cortical layers with the corresponding densities of asymmetric synapses (13). Because the majority (about 85%) of asymmetric synapses in cat area 17 are on dendritic spines (14), the asymmetric synapse densities and the volume densities of dendritic spines should be roughly equal. This is illustrated in Fig. 1*B*. No significant differences can be seen between the volume densities of dendritic spines and densities of asymmetric synapses (green points in Fig. 1*B*) in any cortical layer. This includes layer 1, in which the difference is large ($0.16 \pm 0.09\ \mu m^{-3}$ vs. $0.28 \pm 0.01\ \mu m^{-3}$), although not statistically significant.

Having verified that our method produces reasonable results, we next estimated the volume density of boutons of excitatory neuron axons. This calculation is similar to that of the volume density of dendritic spines. Because the axons of excitatory neurons in our data set are truncated, we could estimate the volume density of boutons only on local axons, that is, axons confined to the domain of the local arbor, as defined by the column of radius *R* (Fig. 1*A*). The results for 2 definitions of locality, $R = 250\ \mu m$ and $R = 500\ \mu m$, are shown in Fig. 1*C*. Layer 2/3 contains the highest density of local boutons, $0.10 \pm 0.02\ \mu m^{-3}$ for $R = 500\ \mu m$. This density decays monotonically toward the deeper layers, similar to the volume density of dendritic spines.

To estimate the overall volume density of boutons (i.e., the volume density of boutons on local and long-range axons), we note that because in cat area 17 most of the boutons on excitatory neuron axons contain only a single asymmetric synapse, this density is approximately equal to the density of asymmetric synapses (14–18). As shown in Fig. 1*C*, the density of local boutons in each layer is only a small fraction of the overall bouton density. Layer 1 contains the highest total density of asymmetric synapses, $0.28 \pm 0.01\ \mu m^{-3}$. In comparison, the volume density of local boutons in layer 1 is $0.018 \pm 0.005\ \mu m^{-3}$ for $R = 500\ \mu m$, which is smaller by 16-fold.

Fig. 1*D* shows how the fractions of local presynaptic terminals on excitatory and inhibitory axons (or excitatory and inhibitory synapses) averaged over the entire cortical depth depend on the local domain radius, *R*. The results illustrate that most of the excitatory synapses near the axis of the columnar domain through the thickness of the cortex come from axons of nonlocal neurons. As an example, if we adopt $R = 500\ \mu m$ as the definition of locality, then a thin column along the axis of the domain [e.g., cortical minicolumn (19)] would contain 26% of the local excitatory synapses. Conversely, 74% of excitatory synapses inside this thin column would originate from nonlocal neurons, i.e., neurons that are located more than 500 μm away from its axis.

This contrast would increase to 18% local versus 82% long range if the definition of locality was based on $R = 250\ \mu m$, which in the cat visual cortex corresponds to the average sizes of ocular dominance (20) or iso-orientation (21, 22) columns. Thus, only about 18% of excitatory synapses near the axes of these columns originate from presynaptic neurons located within the column's range. This fraction will further reduce toward the periphery of the columns. In contrast, the fractions of local inhibitory synapses are significantly higher due to the more compact morphology of inhibitory basket cell axonal arbors. Fig. 1*D* shows that 66% of inhibitory synapses near the axis of $R = 250\ \mu m$ cortical column are local, and only about 34% originate from presynaptic inhibitory basket cells, whose somata are located outside the column.

Connectivity Inside a Cortical Tissue Section. The large spatial extent of arbors of cortical neurons may lead to significantly reduced connectivity in cortical tissue sections. The amount of reduction, or tissue slicing artifact, is particularly strong in thin sections, such as those used for optical imaging. Inevitably, tissue slicing affects neurons located superficially in the section, that is, neurons typically used for electrophysiological recordings. We calculated the fractions of presynaptic boutons and postsynaptic dendritic spines on excitatory neurons that remain connected to the cell bodies of their origin. We refer to such presynaptic and postsynaptic terminals and synaptic connections between them as intact terminals and intact synapses. Consider a typical $D = 300\ \mu m$ cortical tissue section whose plane is perpendicular to the cortical surface (e.g., a coronal section), as illustrated in Fig. 2*A*. Such cortical sections are often used in electrophysiology experiments (12). Within this section, some axonal and dendritic

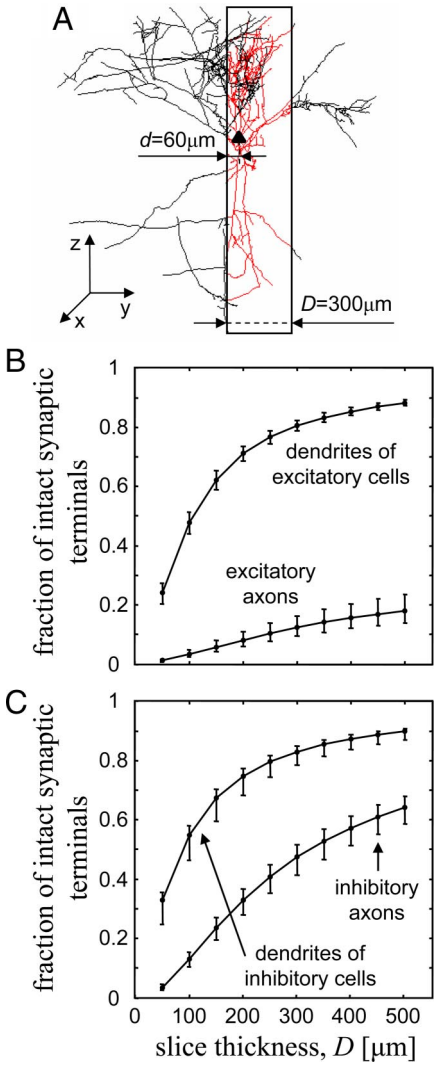

Fig. 2. Fractions of intact presynaptic and postsynaptic terminals in a cortical tissue section. (*A*) Example of a local axonal arbor of a layer 2/3 pyramidal cell. The neuron (black triangle) is located $d = 60$ μm deep inside a model of a $D = 300$-μm-thick cortical section (rectangle). The *z*-axis points in the direction of the pia, and the *y*-axis is perpendicular to the surface of the section. Axonal branches cut due to slicing are shown in black; axons that survived after slicing are shown in red. Note that severed branches are often found inside the section. (*B*) Fractions of intact presynaptic and postsynaptic terminals of excitatory neurons in cortical tissue sections of different thicknesses. (*C*) Fractions of intact presynaptic and postsynaptic terminals of inhibitory basket cells. Error bars indicate 95% CIs.

branches and the synapses that they carry have been severed from the cell bodies of neurons and may no longer be functional. Such branches may originate from neurons whose somata are located outside the boundaries of the section, as well as from neurons within the section (Fig. 2*A*). In the latter case, some neurites located inside the section remained intact (red branches in Fig. 2*A*), whereas others that wander outside and back into the section were truncated (black branches inside the section).

To estimate the fraction of intact postsynaptic terminals on dendrites of excitatory neurons, we first tiled the cortex horizontally with the reconstructions of dendrites of excitatory cells. Next, we truncated dendritic branches *in silico* to imitate the effect of tissue slicing, and calculated the fraction of postsynaptic terminals that remained intact (for details, see SI Text). This fraction is an increasing function of the section thickness (Fig.

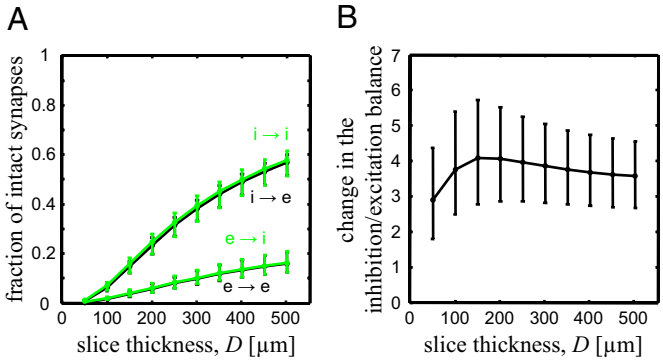

Fig. 3. Fractions of intact synapses in a cortical tissue section. (*A*) Estimated fractions of intact synaptic connections among excitatory neurons (e) and inhibitory basket cells (*i*) in cortical tissue sections of different thicknesses. Curves for all 4 types of connections are shown. Severed synapses may originate from neurons located inside or outside of the section. (*B*) Change in the inhibition–excitation balance in cortical tissue sections of different thicknesses. This change is calculated as the ratio between the fractions of intact i→e and e→e synapses (black curves in *A*). Error bars indicate 95% CIs.

2*B*); it is about 0.8 in a $D = 300$-μm cortical section of cat area 17. We used a slightly different approach to estimate the fraction of intact presynaptic terminals on excitatory neuron axons. Again, we tiled the cortex horizontally with the reconstructions of excitatory neuron axons. We then truncated these axons to the boundaries of the section and calculated the expected number of intact presynaptic terminals on these axons. To estimate the fraction of intact presynaptic terminals, we divided this number by the expected number of asymmetric synapses in a section of that thickness. The results of this calculation (Fig. 2*B*) illustrate just how nonlocal the excitatory axons are; the fraction of intact presynaptic terminals is only about 12% in a $D = 300$-μm cortical section and about 18% in a 500-μm-thick section.

Fig. 2*C* shows the average fractions of intact synaptic terminals on axons and dendrites of inhibitory basket cells in cortical sections of different thicknesses. As expected, the fraction of intact synaptic terminals on dendrites does not differ significantly between inhibitory basket cells and excitatory cells (Fig. 2*B*), because of similar dendritic arbor sizes. The fraction of intact presynaptic terminals on basket cell axons is significantly smaller, but much higher than that for excitatory axons, which are the most affected by the slicing artifact due to their long-range nature.

The fractions of intact synapses can be estimated by multiplying the fractions of intact presynaptic and postsynaptic terminals. Fig. 3*A* shows the results for 4 types of connections among the excitatory (e) and inhibitory (*i*) neurons. Because the fractions of intact synaptic terminals on dendrites of excitatory and inhibitory neurons do not differ significantly (Fig. 2 *B* and *C*), the difference in the fraction of intact synapses (Fig. 3*A*) is due mainly to the presynaptic neuron type. The fraction of intact synapses is significantly larger for presynaptic inhibitory basket cells than for presynaptic excitatory neurons. In a $D = 300$-μm-thick cortical section, the fraction of intact inhibitory synapses is about 0.38, whereas the fraction of intact excitatory synapses is only 0.10. This differential reduction in the number of intact synapses results from morphological differences in the excitatory and inhibitory basket cell axonal arbors. We define the balance between excitation and inhibition in a cortical tissue section as the ratio between the fractions of intact inhibitory and excitatory synapses. For a wide range of section thicknesses, this balance is shifted toward inhibition by roughly 4-fold (Fig. 3*B*). In a $D = 300$-μm-thick cortical section, the excitation–inhibition balance is shifted by a factor of 3.8.

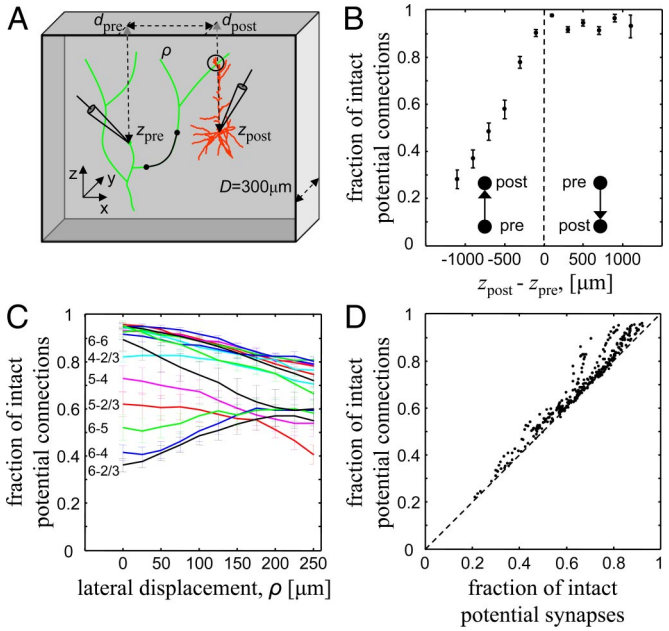

Fig. 4. Connectivity of excitatory neuron pairs in a cortical tissue section. (*A*) Schematic of a presynaptic axon (green) and a postsynaptic dendrite (red) in a model of a $D = 300$-μm-thick cortical section (rectangular prism). Neuron pairs connected in vivo (black circle) may be disconnected due to slicing if the synaptic connection is located outside the section and/or if axonal or dendritic branches carrying the synapse wander outside the section boundaries (black axonal segment). (*B*) Fraction of intact potential connections for pairs of vertically aligned excitatory neurons ($\rho = 0$) plotted against the difference in their laminar positions, z_{post} - z_{pre}. The left half of the figure corresponds to situations where the presynaptic cell is located deeper in the cortex than the postsynaptic cell, and the right half corresponds to the opposite ordering. (*C*) Fraction of intact potential connections for pairs of excitatory neurons located in different layers plotted as function of the lateral displacement between the neurons, ρ. All neurons are positioned 60 μm deep in the section. Each line corresponds to a different projection between cortical layers 2/3, 4, 5, and 6. Curves for all 16 projections are plotted, but some of the curves are not labeled, to avoid clatter. (*D*) Fraction of intact potential connections is correlated with the fraction of intact potential synapses between neurons. Individual points correspond to neuron pairs from different cortical layers at different lateral displacements. Error bars in *B* and *C* indicate SEs of the mean values.

Tissue slicing artifact also affects the connectivity between pairs of neurons whose somata are located in the cortical tissue section. Consider a pair-recording experiment performed in a $D = 300$-μm-thick cortical section. In this experiment, dual sharp or whole-cell recordings were made from neurons located superficially in the section in an effort to identify synaptically connected neuron pairs (Fig. 4*A*). The results give the probabilities of finding connected pairs of neurons (see ref. 12 for a review), as well as the number of synapses per connection (11). They also can be used to construct interlaminar cortical connectivity diagrams (12, 23). But how representative are such diagrams of the in vivo connectivity? It is obvious that the number of synapses between a pair of synaptically connected neurons in the section may be reduced compared with that in vivo (Fig. 4*A*).

If actual synapses between a pair of synaptically connected neurons are established probabilistically from the set of available potential synapses (24), then the reduction in the number of actual synapses is directly related to the reduction in the number of potential synapses. A potential synapse is a location in the neuropil in which an axon of a presynaptic neuron and a dendrite of a postsynaptic neuron are close enough (within distance s) to allow the formation of an actual synapse between the neurons. The distance s depends on the types of synapses that can exist between the branches. For synapses on spines considered here, this distance is on the order of the average spine length, typically 1–2 μm (25–27). In all of our numerical calculations, we used a value of $s = 2$ μm. Because the expected number of potential synapses between neurons scales linearly with distance s (10), and because here we report only relative fractions of potential synapses, the exact value of the parameter s does not affect our results.

We next evaluated the effect of tissue slicing on the probability of potential connectivity and on the mean number of potential synapses between pairs of excitatory neurons (for details, see *SI Text*). We found that in a $D = 300$-μm-thick cortical section, the fraction of potential connections which remain intact after tissue slicing depends strongly on the laminar positions of the presynaptic and postsynaptic neurons. Fig. 4*B* shows how the fraction of intact potential connections for pairs of vertically aligned excitatory neurons located $d_{pre} = d_{post} = 60$ μm deep in the section depends on the difference in their laminar positions, z_{post} - z_{pre}. If the presynaptic neuron is located more superficially than the postsynaptic neuron (*Right*), then potential connectivity is reduced only slightly, to about 94%. Conversely, the fraction of intact potential connections decreases progressively with increasing distance between the cells. This effect is strongest for projecting neurons of layers 6 to 2/3, where the probability of observing potentially connected pairs of excitatory neurons drops to about 28% of the in vivo value. The asymmetric reduction of potential connectivity between descending and ascending projections results from the shapes of axonal arbors (Fig. S1). For example, the descending axons of layer 2/3 and layer 4 excitatory neurons are primarily vertical and form perpendicular axon collaterals that extend laterally only after reaching the target layer, but in contrast, deep-layer neurons in cat area 17 [but not in monkey (28)] tend to have axons that ascend along diagonal trajectories and are affected more strongly by tissue slicing.

Fig. 4*C* shows how the fraction of intact potential connections for different interlaminar projections depends on lateral displacement between the excitatory neurons. The strongest reduction can be seen for projecting neurons of layers 6 to 2/3, located on top of one another, closely followed by reductions in projecting neurons of layers 6 to 4, 6 to 5, 5 to 2/3, and 5 to 4. In general, the fraction of intact potential connections decreases with increasing lateral separation, ρ, between the neurons. Exceptions to this rule include the projections from layer 6 to layers 2/3, 4, and 5, which show an opposite trend. We obtained results very similar to those shown in Fig. 4*B* and *C* for the fraction of intact potential synapses (data not shown). This similarity arises from the fact that the fraction of intact potential connections is strongly correlated with the fraction of intact potential synapses for all of the pairs of excitatory neurons evaluated, that is, neurons from different cortical layers and different lateral displacements, ρ, in the 0–250 μm range (Fig. 4*D*).

Discussion

Insight into basic details of cortical connectivity, such as those explored in this study, is of great importance to both the computational and experimental neuroscience communities. We found that excitatory connectivity in cat area 17 is highly nonlocal; 74% of excitatory synapses near the axis of a 1,000-μm-diameter cortical column come from neurons located outside the column. Although we are not yet able to delineate the contributions from different sources to these long-range synapses, our results give a sense of how strongly interconnected cortical columns must be with one another, as well as with the structures of remote regions.

Validation of Our Results. Our results rely on a set of reconstructed neurons, as well as on the anatomical parameters obtained from previously published studies. We conducted 2 tests to validate our results. First, we compared the volume density of spines on excitatory neuron dendrites derived from our analysis with the density of asymmetric synapses (Fig. 1*B*), and found that the 2 densities were statistically similar in all layers. Second, we compared the total length of axonal and dendritic processes in a unit volume of neuropil (length density of neurites) calculated based on our data with that from the electron microscopic study of Foh *et al.* (29). In that study, the combined length density of axons and dendrites, 3.8 ± 0.3 μm/μm^3, was measured near the layer 3/4 border of the cat visual cortex. Based on our set of reconstructed neurons and anatomical data set, we estimated the following composition of length density near the layer 3/4 border: axons of excitatory cells, 3.7 ± 0.8 μm/μm^3; dendrites of excitatory cells, 0.36 ± 0.08 μm/μm^3; inhibitory basket cell axons, 0.23 ± 0.04 μm/μm^3; and inhibitory basket cell dendrites, 0.032 ± 0.009 μm/μm^3. Adding together these 4 contributions, we arrived at a total length density of 4.3 ± 0.8 μm/μm^3, which is not significantly different than the estimate of Foh *et al.* (29). This result would not be expected to change significantly if the length densities of other GABAergic cells classes were added, because inhibitory basket cells near the layer 3/4 border already account for the majority of GABAergic cells (3).

Comparison With Other Studies. Our findings are closely related to those reported by Binzegger *et al.* (3), who analyzed a data set of neurons reconstructed from cat area 17 of similar size and composition to our data set. Among other calculations, Binzegger *et al.* counted the total numbers of synaptic terminals on excitatory axons in different cortical layers of area 17 and compared them with the numbers of asymmetric synapses reported by Beaulieu and Colonnier (13). They found good agreement between the synapse counts in layers 2/3 and 5; however, in layers 1, 4, and 6, their predicted numbers of synapses were substantially lower than the actual numbers of asymmetric synapses. One likely reason for the missing synapses, or the "dark matter of the cortex," is missing pathways remaining to be discovered. Overall, the fraction of missing synapses in area 17 was on the order of 40%. Making a direct comparison of our results with those of Binzegger *et al.* (3) is difficult, because we limited the analysis of axonal arbors of excitatory neurons to the local arbor domains (with a maximum radius of 500 μm), where the density of branches could be estimated reliably, whereas Binzegger *et al.* truncated the axonal arbors to different extents (often much larger than 1,000 μm) during the reconstruction process. We found a fraction of missing synapses of 66%–79% [95% confidence interval (CI)] for the largest considered extent of the local arbor domain (radius of 500 μm), significantly higher than the value reported by Binzegger *et al.* This discrepancy may be accounted for by extending the size of the local arbor domain beyond 500 μm. Differences in methodologies and data sets of reconstructed neurons could contribute to this discrepancy as well.

In the rat hippocampus, differences in the extent of axonal arborizations of excitatory and inhibitory cells have been well studied (31, 32). In agreement with our results, it has been estimated that in hippocampal slices, 80%–90% of excitatory synapses may be truncated (33), whereas inhibitory basket cell synapses remain relatively unaffected. As a result, the balance between excitation and inhibition in the in vitro hippocampal slice preparation is unnaturally modified.

Implications of Our Results. Our findings have several immediate implications. First, electrophysiological studies conducted in cortical tissue sections may significantly underestimate the extent of cortical connectivity. For example, we estimated that the reported probabilities of finding connected nearby neuron pairs in sections (typically about 10%) and the expected numbers of actual synapses per pair of synaptically connected neurons may understate the in vivo numbers by as much as 3-fold for some projections. Second, due to the uneven reduction in the numbers of intact excitatory and inhibitory synapses in cortical tissue sections, the balance between excitation and inhibition is shifted by a factor of 3.8 toward inhibition. Although the cut axons will remain spontaneously active, cortical tissue sections may appear less excitable than in vivo. This observation possibly could explain the need to use modified low-magnesium artificial cerebrospinal fluid in some electrophysiological experiments performed in cortical tissue sections (34). Third, our results provide a quantitative foundation for estimating interactions in vivo, which can come from remote cortical locations, such as excitatory and inhibitory influences from beyond the classical receptive fields (35–37). Finally, computational models of cortical connectivity often underestimate the extent of long-range connectivity. Motivated by the notion of structural columns [e.g., minicolumns (19, 38, 39)] and functional columns [e.g., orientation and ocular dominance (40)] in the cortex, such models often assume that the majority of synaptic connections are made within columnar units (roughly 500 μm in diameter; see, e.g., ref. 41) that are only weekly interconnected with one another. Our results argue against such columnar organization of connectivity in cat area 17. Based on the analysis of limited data sets of neurons from different species and cortical areas, we believe that the long-range nature of connectivity observed in cat area 17 may be a dominant characteristic of cortical connectivity in general. Future experiments are needed to test this hypothesis and provide the quantitative fractions of long-range synapses in different cortical systems.

Materials and Methods

Experimental Procedures. Details of the labeling and reconstruction of the neurons used in this study have been described previously (2, 42, 43). In brief, excitatory neurons and inhibitory basket cells from adult cat area 17 were labeled in vivo either intracellularly or retrogradely and reconstructed in 3 dimensions with the Neurolucida system (MicroBrightField) from multiple adjoining sections. Soma positions and cortical laminar boundaries were marked during the reconstruction process. All reconstructions were corrected for tissue shrinkage and conformed to a common cortical template of cat area 17 (Fig. S1). The latter was determined by minimizing the mean squared distortion arising from piecewise-linear conformation of tissue sections from individual animals to this template. Although neuron reconstructions were done from large blocks of tissue, many axonal branches of excitatory neurons were truncated because of tissue slicing. The densities of some reconstructed excitatory axons beyond a lateral extent of $R = 500$ μm (the cylindrical domain through the thickness of the cortex in Fig. 1*A*) were deemed unreliable; thus, we restricted the analysis of all excitatory axonal arbors to the domains of their local arbors ($R \leq 500$ μm). We reconstructed the axons of inhibitory basket cells and the dendritic arbors of all of the neurons in their entirety.

Anatomical Data From Other Studies. Our results rely on a number of anatomical parameters of adult cat area 17, most of which were adopted from previously published studies. Unless stated otherwise, all of the data are given as mean $\pm$ SD.

The densities of excitatory neurons and inhibitory basket cells in different cortical layers were calculated as described by Binzegger *et al.* (3). The total numbers of neurons per 1 mm^3 in layers [1, 2/3, 4, 5, and 6] of cat area 17 were obtained from the work of Beaulieu and Colonnier (44), who measured the densities of neurons in the monocular and binocular regions of area 17 in $n = 6$ adult cats. The measurements in each animal were corrected for tissue shrinkage. Only layer 4 exhibited any significant difference between the monocular and binocular regions. Because we did not have complete information regarding the monocular or binocular origin of the cells in our data set, we averaged the densities for the 2 regions, resulting in $[0.73 \pm 0.2, 5.8 \pm 0.4, 5.9 \pm 0.5, 4.2 \pm 0.5, 6.3 \pm 0.6] \times 10^4$ mm^{-3}. According to the study of Gabbott and Somogyi (45), performed in area 17 of $n = 5$ adult cats, GABAergic cells comprised [0.97, 0.22, 0.20, 0.18, 0.17] fractions of all neurons. The density of excitatory neurons was estimated as the difference between the overall

density of neurons and the density of GABAergic cells, resulting in [0.022 ± 0.005, 4.5 ± 0.3, 4.8 ± 0.4, 3.4 ± 0.4, 5.3 ± 0.5] × 10^4 mm^{-3}.

Inhibitory basket cells in layers [2/3, 4, 5] are estimated to account for [0.42, 0.78, 0.42] of all GABAergic cells (3) (see, however, ref. 30, in which this estimate is 0.25–0.35 in layer 4), resulting in densities of basket cells in these layers of [0.54 ± 0.04, 0.93 ± 0.07, 0.32 ± 0.03] × 10^4 mm^{-3}. It should be noted that layer 1 is free of basket cells. For layer 6, our literature search provided no reliable estimate on the density of basket cells; thus, all of the results related to basket cells are based on data from layers 1–5, which together comprise almost 80% of the cortical thickness.

We derived the densities of asymmetric synapses from the work of Beaulieu and Colonnier (13), who measured the densities of asymmetric synapses in different layers in monocular and binocular regions in area 17 of $n = 6$ adult cats. The results were corrected for tissue shrinkage. We averaged the densities of asymmetric synapses in the monocular and binocular regions, because the differences between the regions were not statistically significant. As a result, the average densities of asymmetric synapses in layers [1, 2/3, 4, 5, 6] were [0.28 ± 0.01, 0.26 ± 0.01, 0.25 ± 0.01, 0.23 ± 0.02, 0.18 ± 0.01] μm^{-3}.

According to an estimate of Binzegger *et al.* (3), the frequency of synaptic terminals on dendrites (i.e., expected number of synapses per 1 μm of dendritic length) is very similar among excitatory neurons and inhibitory basket cells in layers 2–6 of cat area 17. We used this estimate, 0.73 ± 0.08 μm^{-1}, for the dendrites of all neurons in this study.

The frequency of synaptic terminals on axons (i.e., expected number of synapses established by axonal terminals onto postsynaptic cells per 1 μm of axonal length) can be very well approximated based on the frequency of boutons. This is because the fractions of multiple synapse boutons on excitatory neurons and inhibitory basket cells in adult cat area 17 generally are very low (14–18). We estimated the bouton frequency by combining results reported previously (46) and our measurements (for details, see SI Text), with both data sets corrected for tissue shrinkage. The results are 0.061 ± 0.010 μm^{-1} for pyramidal cells in layer 2/3 ($n = 11$ cells), 0.068 ± 0.024 μm^{-1} for spiny stellate and pyramidal cells in layer 4 ($n = 10$ cells), 0.051 ± 0.007 μm^{-1} for pyramidal cells in layer 5 ($n = 4$ cells), 0.097 ± 0.033 μm^{-1} for pyramidal cells in layer 6 ($n = 7$ cells), 0.105 ± 0.018 μm^{-1} for basket cells in layer 2/3 ($n = 13$ cells), 0.110 ± 0.010 μm^{-1} for basket cells in layer 4 ($n = 8$ cells), and 0.076 ± 0.013 μm^{-1} for basket cells in layer 5 ($n = 2$ cells).

ACKNOWLEDGMENTS. Support for this work was provided by National Institutes of Health Grants NS047138 and NS063494 (to A.S.). L.M. was supported by the European Regional Development Fund (CONSOLIDER CSD2007-00023), by National Institutes of Health Grant EY09593 to Judith A. Hirsch, and by Spanish Ministry of Education and Science Grant BFU2007-67834. Z.K. was supported by Deutsche Forschungsgemeinschaft Grant DFG-SFB509/TPA6, European Community Grant FP6-2004-IST-FETPI/15879, and Hungarian Academy of Sciences and the University of Debrecen Grant MTA-DE TKI242. We thank Judith Hirsch from the University of Southern California for the insightful comments on the manuscript and for making the data set of neurons reconstructed in her laboratory available for this project. We also thank Drs. Péter Buzás and Krisztina Kovács, Ruhr-Universität Bochum for their neuron reconstructions.

1. Ramón y Cajal S, Pasik P, Pasik T (1999) *Texture of the Nervous System of Man and the Vertebrates* (Springer, New York), Vol 3, pp. 185–279.
2. Stepanyants A, *et al.* (2008) Local potential connectivity in cat primary visual cortex. *Cereb Cortex* 18:13–28.
3. Binzegger T, Douglas RJ, Martin KA (2004) A quantitative map of the circuit of cat primary visual cortex. *J Neurosci* 24:8441–8453.
4. Gilbert CD, Wiesel TN (1989) Columnar specificity of intrinsic horizontal and corticocortical connections in cat visual cortex. *J Neurosci* 9:2432–2442.
5. Callaway EM, Katz LC (1990) Emergence and refinement of clustered horizontal connections in cat striate cortex. *J Neurosci* 10:1134–1153.
6. Kisvárday ZF, Eysel UT (1992) Cellular organization of reciprocal patchy networks in layer III of cat visual cortex (area 17). *Neuroscience* 46:275–286.
7. Hirsch JA, Gallagher CA, Alonso JM, Martinez LM (1998) Ascending projections of simple and complex cells in layer 6 of the cat striate cortex. *J Neurosci* 18:8086–8094.
8. Kisvárday ZF, *et al.* (2002) One axon-multiple functions: Specificity of lateral inhibitory connections by large basket cells. *J Neurocytol* 31:255–264.
9. Shepherd GM, Stepanyants A, Bureau I, Chklovskii D, Svoboda K (2005) Geometric and functional organization of cortical circuits. *Nat Neurosci* 8:782–790.
10. Stepanyants A, Chklovskii DB (2005) Neurogeometry and potential synaptic connectivity. *Trends Neurosci* 28:387–394.
11. Markram H, Lübke J, Frotscher M, Roth A, Sakmann B (1997) Physiology and anatomy of synaptic connections between thick tufted pyramidal neurones in the developing rat neocortex. *J Physiol* 500(Pt 2):409–440.
12. Thomson AM, Lamy C (2007) Functional maps of neocortical local circuitry. *Frontiers Neurosci* 1:19–42.
13. Beaulieu C, Colonnier M (1985) A laminar analysis of the number of round-asymmetrical and flat-symmetrical synapses on spines, dendritic trunks, and cell bodies in area 17 of the cat. *J Comp Neurol* 231:180–189.
14. Kisvárday ZF, *et al.* (1986) Synaptic targets of HRP-filled layer III pyramidal cells in the cat striate cortex. *Exp Brain Res* 64:541–552.
15. Gabbott PL, Martin KA, Whitteridge D (1987) Connections between pyramidal neurons in layer 5 of cat visual cortex (area 17). *J Comp Neurol* 259:364–381.
16. Anderson JC, Douglas RJ, Martin KA, Nelson JC (1994) Synaptic output of physiologically identified spiny stellate neurons in cat visual cortex. *J Comp Neurol* 341:16–24.
17. Buhl EH, *et al.* (1997) Effect, number and location of synapses made by single pyramidal cells onto aspiny interneurones of cat visual cortex. *J Physiol* 500(Pt 3):689–713.
18. Somogyi P, Kisvárday ZF, Martin KA, Whitteridge D (1983) Synaptic connections of morphologically identified and physiologically characterized large basket cells in the striate cortex of cat. *Neuroscience* 10:261–294.
19. Mountcastle VB (1997) The columnar organization of the neocortex. *Brain* 120(Pt 4):701–722.
20. Kaschube M, *et al.* (2003) The pattern of ocular dominance columns in cat primary visual cortex: Intra- and interindividual variability of column spacing and its dependence on genetic background. *Eur J Neurosci* 18:3251–3266.
21. Kaschube M, Wolf F, Geisel T, Löwel S (2002) Genetic influence on quantitative features of neocortical architecture. *J Neurosci* 22:7206–7217.
22. Rao SC, Toth LJ, Sur M (1997) Optically imaged maps of orientation preference in primary visual cortex of cats and ferrets. *J Comp Neurol* 387:358–370.
23. Thomson AM, Bannister AP (2003) Interlaminar connections in the neocortex. *Cereb Cortex* 13:5–14.
24. Stepanyants A, Hof PR, Chklovskii DB (2002) Geometry and structural plasticity of synaptic connectivity. *Neuron* 34:275–288.
25. Peters A, Kaiserman-Abramof IR (1970) The small pyramidal neuron of the rat cerebral cortex: The perikaryon, dendrites and spines. *Am J Anat* 127:321–355.
26. Spacek J, Hartmann M (1983) Three-dimensional analysis of dendritic spines, I: Quantitative observations related to dendritic spine and synaptic morphology in cerebral and cerebellar cortices. *Anat Embryol* 167:289–310.
27. Anderson JC, Douglas RJ, Martin KA, Nelson JC (1994) Map of the synapses formed with the dendrites of spiny stellate neurons of cat visual cortex. *J Comp Neurol* 341:25–38.
28. Callaway EM (1998) Local circuits in primary visual cortex of the macaque monkey. *Annu Rev Neurosci* 21:47–74.
29. Foh E, Haug H, Konig M, Rast A (1973) [Determination of quantitative parameters of the fine structure in the visual cortex of the cat, also a methodological contribution on measuring the neuropil (author's transl)]. *Microsc Acta* 75:148–168.
30. Budd JM (2000) Inhibitory basket cell synaptic input to layer IV simple cells in cat striate visual cortex (area 17): A quantitative analysis of connectivity. *Vis Neurosci* 17:331–343.
31. Sik A, Penttonen M, Buzsáki G (1995) Hippocampal CA1 interneurons: An in vivo intracellular labeling study. *European J Neurosci* 15:6651–6665.
32. Freund TF, Buzsaki G (1996) Interneurons of the hippocampus. *Hippocampus* 6:347–470.
33. Sík A (2006) Merging structure and function: Combination of In vivo extracellular and intracellular electrophysiological recordings with neuroanatomical techniques, *Neuroanatomical Tract-Tracing 3: Molecules, Neurons, and Systems*. eds. Záborszky L, Wouterlood FG, Lanciego JL (Springer, New York), p 175.
34. Sanchez-Vives MV, McCormick DA (2000) Cellular and network mechanisms of rhythmic recurrent activity in neocortex. *Nat Neurosci* 3:1027–1034.
35. Allman J, Miezin F, McGuinness E (1985) Stimulus-specific responses from beyond the classical receptive field: Neurophysiological mechanisms for local–global comparisons in visual neurons. *Annu Rev Neurosci* 8:407–430.
36. Gilbert CD, Wiesel TN (1990) The influence of contextual stimuli on the orientation selectivity of cells in primary visual cortex of the cat. *Vision Res* 30:1689–1701.
37. DeAngelis GC, Freeman RD, Ohzawa I (1994) Length and width tuning of neurons in the cat's primary visual cortex. *J Neurophysiol* 71:347–374.
38. Peters A, Payne BR (1993) Numerical relationships between geniculocortical afferents and pyramidal cell modules in cat primary visual cortex. *Cereb Cortex* 3:69–78.
39. Rockland KS, Ichinohe N (2004) Some thoughts on cortical minicolumns. *Exp Brain Res* 158:265–277.
40. Hubel DH, Wiesel TN (1977) Ferrier lecture: Functional architecture of macaque monkey visual cortex. *Proc R Soc London Ser B* 198:1–59.
41. Markram H (2006) The blue brain project. *Nat Rev Neurosci* 7:153–160.
42. Buzás P, Eysel UT, Kisvárday ZF (1998) Functional topography of single cortical cells: an intracellular approach combined with optical imaging. *Brain Res Protoc* 3:199–208.
43. Hirsch JA, Alonso JM, Reid RC, Martinez LM (1998) Synaptic integration in striate cortical simple cells. *J Neurosci* 18:9517–9528.
44. Beaulieu C, Colonnier M (1983) The number of neurons in the different laminae of the binocular and monocular regions of area 17 in the cat, Canada. *J Comp Neurol* 217:337–344.
45. Gabbott PL, Somogyi P (1986) Quantitative distribution of GABA-immunoreactive neurons in the visual cortex (area 17) of the cat. *Exp Brain Res* 61:323–331.
46. Anderson JC, Binzegger T, Douglas RJ, Martin KA (2002) Chance or design? Some specific considerations concerning synaptic boutons in cat visual cortex. *J Neurocytol* 31:211–229.